Numerical Investigation of Mass Transfer with Two-Phase Slug Flow in a Capillary

Wei Han[1], Brian H. Dennis[*,1]
University of Texas at Arlington
*Department of Mechanical and Aerospace, University of Texas at Arlington, Arlington, 76019

Abstract: The multiphase flow of two immiscible liquids in a circular capillary micromixer was investigated numerically. The mass transfer characteristics of this flow pattern are of primary interest in this study. A simple neutralization titration reaction was chosen as the basis. The liquid-liquid two phase slug flow was formed during the mixing. The mixing was quantified for different volume flow rates of the reactants. To simplify the computational procedure, instead of applying different volume flow rate, the wall was moved with different average slug flow velocity. It was shown that the residence time required for reaction completeness was dominated by the average flow velocity for this type of micromixer. Furthermore, a parametric two-dimensional model was implemented with COMSOL Multiphysics to investigate mixing phenomenon within the slugs. The COMSOL model allows for rapid analysis of different microchannel geometries and flow rates. The results show a dramatic intensification of the reaction as the aspect ratio, which is the ratio of slug length to capillary radius, decreases with a constant average flow velocity.

Keywords: Slug flow, Liquid-liquid, Two-phase, Mass transfer, COMSOL Multiphysics

1. Introduction

Slug flow is a type of two-phase flow pattern formed either inside capillary or microchannel. There are two major types of slug flow: gas-liquid and liquid-liquid two phase flow. Slug flow has been widely used in biomedical and engineering applications, which is due to the intensification of heat and mass transfer with the large ratio of surface-to-volume and the internal circulation within slugs in micro scale.

Burns and Ramshaw [8] presented the intensification of mass transfer with slug flow in a capillary channel with a simple titration reaction. The details of slug generation, slug size and pressure drop were described by Kashid and Agar [9] with a capillary microreactor. The quantitative study of the mass transfer with two immiscible fluids in a T-shaped microchannel system has been investigated by Zhao et al. [10]. A great of study has proved that the slug flow plays an important role in the process of mass transfer in microsystem.

With the development and application of MEMS technology, the micro scale reactor has become the new topic in chemical engineering and biotechnology fields. It has been proved that microreactor technology provides potential benefits to processing technology, especially in chemical reaction engineering [1]. The benefits of the microreactor are not only decreasing the mixing time but also enhancing the heat and mass transfer [2]. A transesterification reaction implemented with a capillary microreactor for catalyzed synthesis of biodiesel shows the significant effect of micro scale reactor in chemical processing [3].

For those applications, the mixing of two phases with chemical reaction is of interest. Moreover, from a practical point of view, increasing of mass transfer efficiency between two insoluble phases will bring plenty of advantage [4]. Zhao et al. [7] experimentally compared parallel flow and slug flow in a rectangular microchannel with different Weber number based on the mass transfer between deionized water and kerosene. A quantitative study of discrete drop mixing in a microchannel demonstrated three types of transport phenomena: diffusion-oriented, dispersion-oriented and convection-oriented, according to different Péclet number [5]. Soleymani et al. [6] computationally investigated the mixing phenomena in a T-type microchannel with low Reynolds number ($Re<250$), as well as, they presented the experiment to prove that the significant effect of vortices in mixing efficiency.

As well as, the numerical analysis with computational fluid dynamics (CFD) tool was applied to study the mass transfer with liquid-liquid slug flow [11-14]. From the strength of numerical simulations, more details will be

investigated in micro scale than the experimental results. Basically, the ability of CFD method is to describe the flow field by solving a set of conservation equations. The concentration of the chemical species and other scalar variable will be also included in the solution of the algebraic equation.

Among those works, in spite of the global mass transfer characteristic in microsystem has been evaluated. However, the details of mass transfer phenomena for liquid-liquid slug flow with chemical reaction kinetics has not been well understood, such as the influence from reaction rate and the specific diffusion coefficient within two different phases, as well as the effect of aspect ratio on the mixing efficiency.

In the present work, the numerical analysis will be performed with COMSOL Multiphsics which is based on Finite Element Method (FEM). To investigate the mixing efficiency and mixing phenomenon inside slugs, the residence time under different flow condition will be studied. The residence time required for 98% conversion of KOH will be quantified with different aspect ratio under a constant average flow velocity. Moreover, the effect of average flow velocity with a fixed size radius will also be presented. The commercial software Tecplot (Tecplot, Inc.) will be used for postprocessing and results visualization.

2. Computation Model

To investigate the flow behavior inside circular capillary, a two dimensional slice of the capillary was to be considered due to the axisymmetric nature of flow. Basically, the computational domain consisted of two adjacent rectangular units which represent the two immiscible phases, one is organic phase and another is aqueous phase, which is due to the characteristic of slug flow formation.

On the other side, it will also reduce computational effort instead of computing the whole series of alternative slugs within a continuous loop. The width and the length of the rectangle represent the radius and the length of each phase, respectively. The computational domain shows as below (Figure 1) while axis z was defined as central axis.

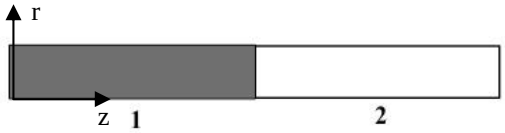

Figure 1. Schematic representation of the computational domain; 1 represents aqueous phase and 2 represents organic phase

In this work, the length of two phases was assumed to be the same due to the same volume flow rate for two fluids and same cross section of passing geometry. The computing scheme was assuming that the slugs were held stationary while the wall of the capillary was moving with a constant velocity which was the average flow velocity.

The different chemical species had to be defined, identified by density and viscosity. To have a better understanding of mass transfer during the slug flow, a simple neutralization titration reaction was implemented as the basis of the study because the reaction takes place without any additional condition and it is easy to be quantified because the ratio of reactants coefficients is 1:1. The chemical reaction equation shows as below (Equation 1):

$$CH_3COOH + KOH \rightarrow CH_3COOK + H_2O \qquad (1)$$

The base (domain 1) was initialized in the aqueous phase to represent potassium hydroxide (KOH) aqueous solution. The mixture of acetic acid (AA) and kerosene was represented by the acid (domain 2) in organic phase.

2.1 Governing Equation

For fluid flow, Navier- Stokes equation (Equation 2, 3) was solved numerically by a finite element method with COMSOL with Matlab 3.5 package. Both phases were assumed incompressible and with Newtonian behavior. The shape and volume of slugs remained same during the mass transfer and chemical reaction. The flow was laminar due to the small Reynolds number. $\vec{u}$ is velocity field which is solved under steady state; ρ and μ are the density and dynamic viscosity, respectively which are constants for both phases; p is pressure which can be solved from the following equations, which are continuity equation (Equation 2) and

conservation of momentum equation (Equation 3).

$$\nabla \cdot \vec{u} = 0 \tag{2}$$

$$\rho(\vec{u} \cdot \nabla)\vec{u} = -\nabla p + \mu \nabla^2 \vec{u} \tag{3}$$

The mass transfer between two phases is governed by the general convection-diffusion equation (Equation 4):

$$\frac{\partial C_{mn}}{\partial t} + \vec{u} \cdot \nabla C_{mn} = \nabla \cdot (D_{mn} \nabla C_{mn}) \pm R_{ij} \tag{4}$$

Where, C_{mn} is the concentration of chemical m in domain n; index $m=2$ represents two chemicals which are AA and KOH, respectively, as well as, index $n=2$ represents two domains which are base phase and acid phase. D_{mn} is diffusion coefficient of solute m in solvent n, which was calculated from Wilke-Chang correlation [15]; R_{ij} is a source term which represents the contribution of chemical reaction; indices i and j represent the two reactants. The reaction is second order irreversible reaction. The reaction rate R_{ij} can be expressed as follow (Equation 5):

$$R_{ij} = kC_iC_j \tag{5}$$

Where, i and j represent two reactants which is AA and KOH; k=0.001m^{3}mol^{-1}s^{-1}, which is kinetic rate constant. Additionally,

$$D_{mn} = 7.4 \times 10^{-8} \frac{T\sqrt{\varphi_n M_n}}{\mu_n (M_m / \rho_m)^{0.6}} \tag{6}$$

Where, D_{mn} is the diffusion coefficient of solute m in solvent n; T is temperature in K; φ_n is the association parameter, value of 2.6 is for aqueous phase, value of 1 for other unassociated solvents, such organic phase; μ_n is the dynamic viscosity of the solvent; ρ_m is the density of solvent; M_m and M_n are the molecular weight of solute and solvent, respectively.

2.2 Simulation Conditions

To solve the convection-diffusion equation numerically, the computations were finished in two stages. First, the velocity profile was obtained by numerically solving the continuity and momentum equations under steady state. The concentration distributions for two domains were obtained by solving the convection-diffusion equation with velocity profile implement.

To the flow filed, the boundary condition at the moving wall was assigned with the average velocity of the fluids. A condition of equal stress, $\mu_1 \frac{\partial u}{\partial r} = \mu_2 \frac{\partial u}{\partial r}$, was applied on the interface of two domains. Furthermore, $r = 0$ was assigned to the central axis to ensure the axial symmetric nature. With regard to the mass transfer, the flux continuity at the interface was satisfied with the following relation:

$$\frac{D_{m1} \partial C_{m1}}{\partial n_1} = D_{m2} \frac{\partial C_{m2}}{\partial n_2}$$

On the moving wall, $\frac{\partial C_{mn}}{\partial \mathbf{n}} = 0$ was assigned, which indicated that no mass flux through the wall, and **n** is the normal vector to the interface. In addition, the periodic boundary was also implemented on the connected interface and r=0 was imposed to the central axis. Moreover, the concentration of two species were initialized at t=0 for domain 1 and domain 2 (base phase and acid phase), which were 250 mol/m^3 and 650 mol/m^3, respectively.

2.3 Mass Transfer

To numerically solve the governing equation, the equations were discretized by using backward differentiation formulas (BDF) method with small time step, as well as, the structured mesh was used to provide higher accuracy. There were totally 3000 elements for entire computation domain. For having better visualization, the entire middle cross section of slugs is shown in Figure 2 and two axes are independent in this plot.

There were two cases have been studied. One case was focused on the pure diffusion mixing phenomenon. In this study case, the mixing of two species was mainly dominated by the diffusion. In the simulation, mass transfer was purely diffusion dominant with the assumption of no velocity field implemented. Therefore, the

concentration profile was obtained by solving diffusion equation (Equation 7) only.

$$\frac{\partial C_{mn}}{\partial t} - \nabla \cdot (D_{mn} \nabla C_{mn}) \pm R_{ij} = 0 \quad (7)$$

As shown in Figure 3, with the assumption of the constant diffusion coefficient and fixed slug length, the time required to reach 98% conversion of KOH is increased with the increase of capillary radius which is characteristic diffusion length, that indicates that the mixing time strongly depends on the size of capillary for the pure diffusion mass transfer.

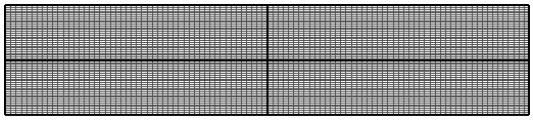

Figure 2. The residence time for reaching 98% conversion of KOH varies with different capillary radius

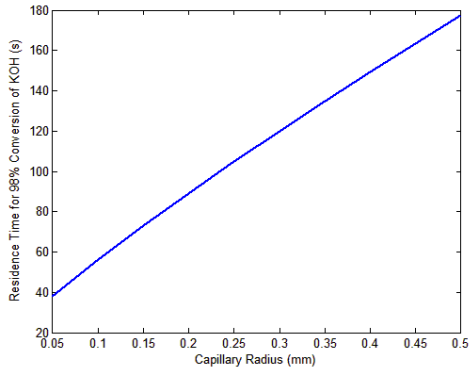

Figure 3. The residence time for reaching 98% conversion of KOH varies with different capillary radius

The second case was the study of passive mixing which was based on solving general convection-diffusion equation. As described earlier, the computational approach was based on solving the N-S equation to obtain the velocity field first and implemented to the general convection-diffusion equation. The flow field was solved under steady state due to the small Reynolds number in two regions. The streamline plot (Figure 3) clearly shows that the internal circulations formed inside both slugs. In this plot, two axes are also independent for better visualization.

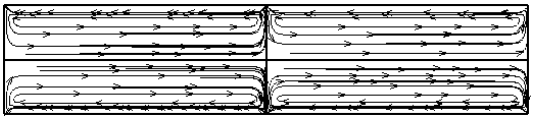

Figure 4. Internal circulation streamline

3. Results

As expected, the mixing time is decreased dramatically with compare to the pure diffusion case with same variation of capillary radius (Figure 5). With the formation of internal circulation within both slugs, the mass is not only transported by diffusion across the interface, the convective mixing is involved as well. With the internal circulation, the interfacial area between two phases is increased and the interfacial concentration is renewed rapidly; furthermore, the molecular diffusion performance is also increased due to the smaller diffusion path within the internal circulation.

As shown in Figure 5, it is found that the time required to obtain 98% conversion of KOH is decreasing while the capillary radius is increasing with fixed slug length and constant average flow velocity. Under the assumption of constant velocity of 0.014m/s and fixed slug length of 4mm, it shows that the aspect ratio has significant effect on the mixing time. The residence time for achieving 98% conversion of KOH increases with increasing the aspect ratio (Figure 6).

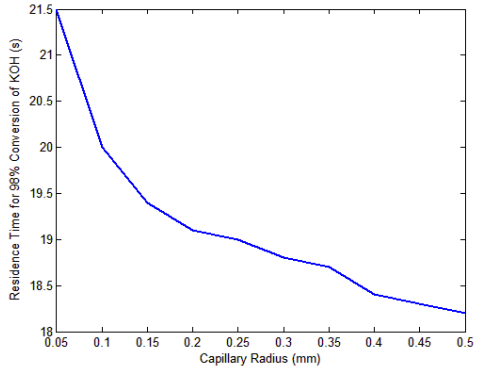

Figure 5. The residence time for reaching 98% conversion of KOH varies with different capillary radius

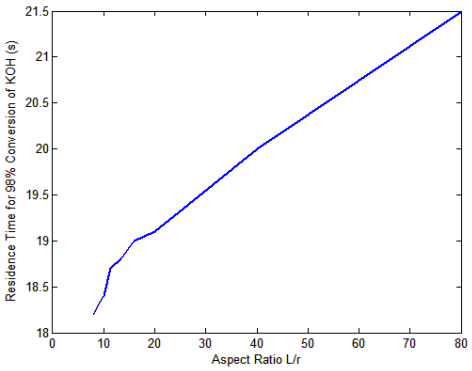

Figure 6. The residence time for reaching 98% conversion of KOH varies with different aspect ratio

Three different cases with aspect ratio of 80, 16 and 8 were focused. The variation of average concentration of two species in two phases verses residence time shows as following (Figure 7, 8 and 9). It clearly shows that the AA is transported into aqueous phase and the reaction mainly takes place within the aqueous phase. Due to the over amount of AA, the concentration of AA will not be vanished on both phases. The concentration of AA approximately becomes equivalent in two phases when the reaction close to equilibrium state.

On the other hand, it also indicates that the mixing rate is getting slower after it reached a certain conversion level. Since the concentrations of two reactants are both decreasing along with time, the reaction rate is decreasing as well. Therefore, it will take longer time to reach the ideal equilibrium after the conversion reached a certain level.

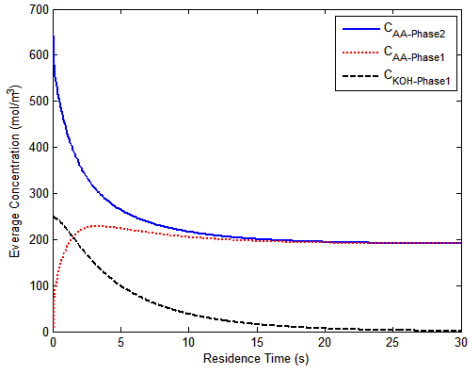

Figure 7. The variation of average concentration of two species at different residence time with aspect ratio 80

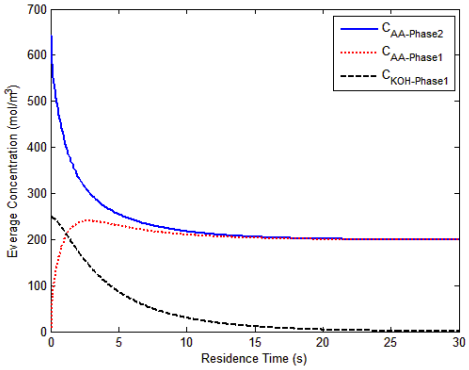

Figure 8. The variation of average concentration of two species at different residence time with aspect ratio 16

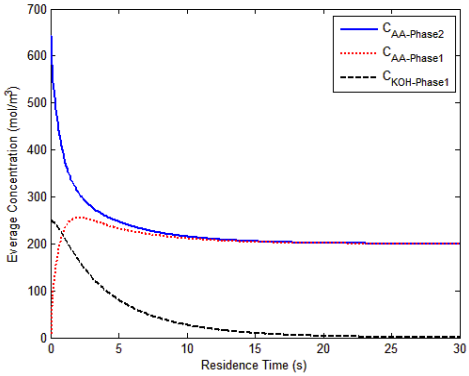

Figure 9. The variation of average concentration of two species at different residence time with aspect ratio 8

Furthermore, different average flow velocity applied with constant capillary radius of 0.25mm and constant slug length of 4mm. It shows that rapid mixing will be obtained with large velocity applied to the moving wall (Figure 10). For this case, the Péclet number is increased which causes the mixing strongly convection dominant. Therefore, the less time will be required to reach 98% conversion of KOH with a fixed size capillary and fixed slug length.

To have bettering understanding of mixing phenomenon, the concentration distributions of KOH in aqueous phase are plotted with different average flow velocities at same time stage (Figure 11). The concentration of KOH in aqueous phase decreased rapidly during mass transfer with reaction under different average

flow velocity. It also indicates that the higher concentration gradient appears at the interface which benefits to the diffusion efficiency at the interfacial area.

The corresponding concentration distributions of AA in two phases at different time stages are also shown as following (Figure 12 and 13), which are under different average flow velocity with fixed aspect ratio of 16. It clearly indicates that the rapid mixing takes place with higher flow rate. The maximum and minimum values of concentration are also shown as following at different time stages. Under velocity of 0.014, 21% of AA has been transported to the aqueous phase in 1s. However, there is only 0.026% of KOH appears in aqueous phase under velocity of 0.002 m/s.

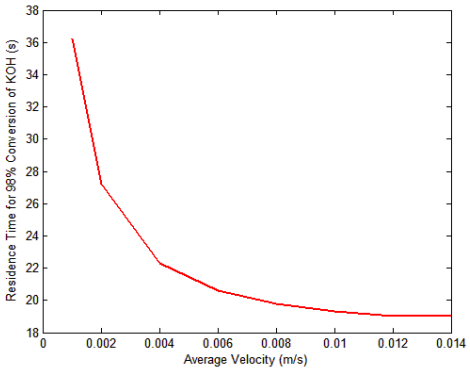

Figure 10. The residence time required to reach 98% conversion of KOH varies with different average flow velocity with aspect ratio of 16

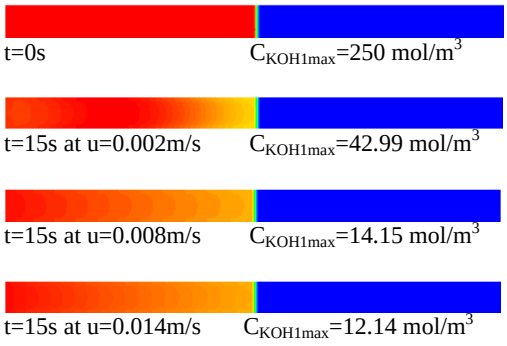

Figure 11. The concentration distribution and maximum concentration value of KOH in domain 1 for different velocity at residence time t=15s

4. Conclusion

The mass transfer with chemical reaction in capillary has been studied with CFD scheme base on FEM method with COMSOL Multiphysics package. The objective is to investigate the effect of capillary size and average flow velocity on the mass transfer with two-phase slug flow. Several simulation cases were carried out for performing the mass transfer behavior under different assumption. It indicates that the significant influence of flow velocity and capillary size on mixing efficiency, as well as, the results show that the higher mixing efficiency obtained with low aspect ratio under constant average flow velocity. With the fixed aspect ratio, the mixing efficiency increases with increasing the average flow velocity.

5. References

1. H. Löwe, W. Ehrfeld, State-of-the-Art in Microreaction Technology: Concepts, Manufacturing and Application, *Electrochimica Acta*, **44**, 3679-3689 (1999)
2. A. Manz, H. Becker, Microsystem Technology in Chemistry and Life Sciences Springer, (1997)
3. J. Sun, J. Ju, L. Ji, L. Zhang, N. Xu, Synthesis of Biodiesel in Capillary Microreactors, *Ind. Eng. Chem. Res*, **47,** 1398-1403 (2008).
4. A. Bhattacharya, General Kinetic Model for Liquid-Liquid Phase-Transfer-Catalyzed Reactions, *Ind. Eng. Chem. Res.* **35**, 645-652 (1996)
5. M. Rhee, M. A. Burns, Drop Mixing in a Microchannel for Lab-on-a-Chip Platforms, *Langmuir*, **24,** 590-601 (2008)
6. A. Soleymani, E. Kolehmainen, I. Turunen, Numerical and Experimental Investigations of liquid mixing in T-type Micromixers, *Chemical Engineering Journal*, **135S,** S219-S228 (2008).
7. Y. Zhao, G. Chen, Q. Yuan, Liquid-Liquid Two-Phase Flow Patterns in a Rectangular Microchannel, *AIChE Journal*, **52,** 4052-4060 (2006)
8. J. R. Burns, C. Ramshaw, the Intensification of Rapid Reactions in Multiphase Systems Using Slug Flow in Capillaries, *Lab on A Chip*, **1**, 10-15 (2001)
9. M. N. Kashid, D. W. Agar, Hydrodynamics of Liquid-Liquid Slug Flow Capillary Microreactor: Flow Regimes, Slug Size and

Pressure Drop, *Chemical Engineering Journal*, **131**, 1-13 (2007)
10. Y. Zhao, G. Chen, Q. Yuan, Liquid-Liquid Two-Phase Mass Transfer in the T-Junction Microchannels, *ALChE Journal*, **53**, 3042-3053 (2007)
11. M. N. Kashid, D.W. Agar, S. Turek, CFD Modelling of Mass Transfer with and without Chemical Reaction in the Liquid-Liquid Slug Flow Microrector, *Chemical Engineering Science*, **62,** 5102-5109 (2007)
12. X. Wang, H. Hirano, N. Okamoto, Numerical Investigation on the Liquid-Liquid, Two Phase Flow in a Y-shaped Microchannel, *ANZIAM J.*, **48,** C963-C976 (2008)
13. M. N. Kashid, D. Fernández Rivas, D. W. Agar, S. Turek, On the Hydrodynamics of Liquid-Liquid Slug Flow Capillary Microreactors, *Asia-Pac. J. Chem. Eng.*, **3**, 151-160 (2008)
14. B. E. Logan, Environmental Transport Processes Wiley- Interscience, (1998)
15. R. S. Brodkey, H. C. Hershey, Transport Phenomena: A Unified Approach, Volume **2**, Brodkey Publishing, (1988)

6. Appendix

Parameter	Symbol	Value
Density of phase 1	ρ_1	998kg/m^3
Density of phase 2	ρ_2	790kg/m^3
Dynamic viscosity of phase 1 (aqueous phase)	μ_1	1.23E-3 Pa·s
Dynamic viscosity of phase 2 (organic phase)	μ_2	2.14E-3 Pa·s
Diffusion Coefficient of AA in aqueous phase	D_{21}	1.30E-9 m^2/s
Diffusion Coefficient of AA in organic phase	D_{22}	1.16E-9 m^2/s
Diffusion Coefficient of KOH in organic phase	D_{12}	1.18E-9 m^2/s

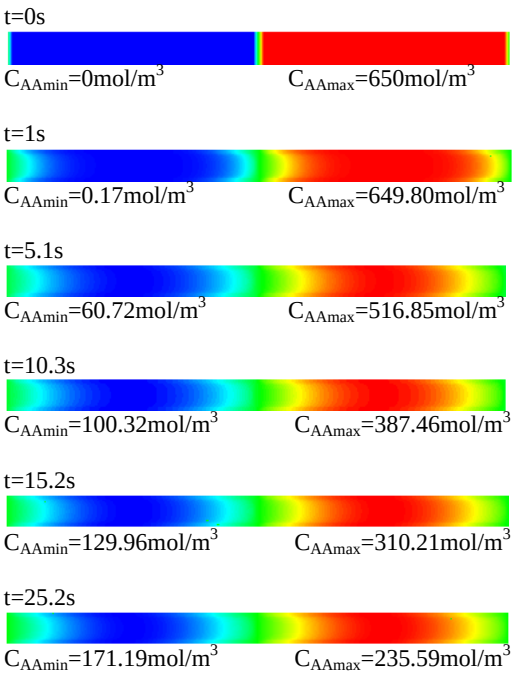

Figure 12. The concentration distribution of AA in two phases under average flow velocity of u=0.002m/s and fixed aspect ratio of 16

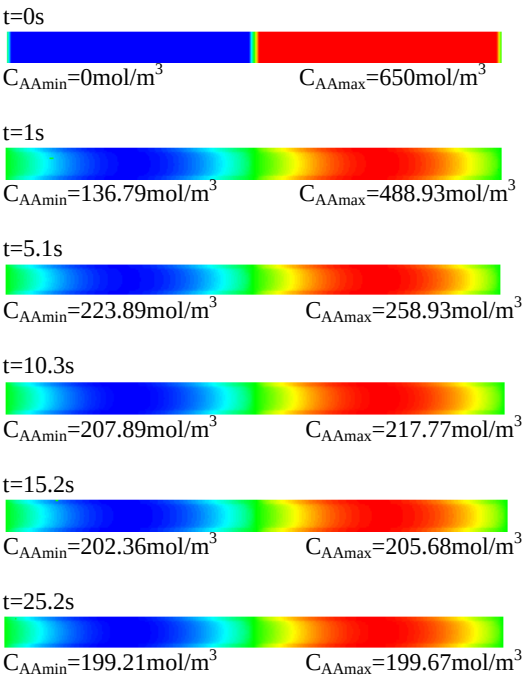

Figure 13. The concentration distribution of AA in two phases under average flow velocity of u=0.014m/s and fixed aspect ratio of 16